ELSEVIER

Materials Science and Engineering A299 (2001) 157–163

MATERIALS SCIENCE & ENGINEERING A

www.elsevier.com/locate/msea

Influence of temperature and strain rate on the flow stress of an FeAl alloy

D.H. Sastry [a,b,*], Y.V.R.K. Prasad [a], S.C. Deevi [b]

[a] *Department of Metallurgy, Indian Institute of Science, Bangalore 560012, India*
[b] *Research Center, Chrysalis Technologies Inc., Richmond, VA 23234, USA*

Received 21 March 2000; received in revised form 26 July 2000

Abstract

The deformation behavior of an FeAl alloy processed by hot extrusion of water atomized powder has been investigated. Compression tests are performed in the temperature range 1073–1423 K and in the strain rate range 0.001–100 s^{-1} up to a true plastic strain of 0.5. The flow stress has been found to be strongly dependent on temperature as well as strain rate. The stress exponent in the power law rate equation is estimated to be in the range 7.0–4.0, decreasing with temperature. The activation energy for plastic flow in the range 1073–1373 K varies from 430 kJ mol^{-1} at low stresses to 340 kJ mol^{-1} at high stresses. However, it is fairly independent of strain rate and strain. The activation area has similarly shown a stress dependence and lies in the range 160–45b^2. At 1423 K and at strain rates lower than 0.1 s^{-1} a strain rate sensitivity of 0.3 is observed with an associated activation energy of 375 kJ mol^{-1}. The plastic flow in the entire range of temperature and strain rate investigated appears to be controlled by a diffusion mechanism. The results have revealed that it is possible to process the alloy by superplastic forming in the range 1373–1423 K at strain rates lower than 0.1 s^{-1}. © 2001 Elsevier Science B.V. All rights reserved.

Keywords: Intermetallics; Iron aluminides; Flow stress; Activation energy for plastic flow; High temperature deformation; Deformation mechanisms; Superplasticity

1. Introduction

Intermetallic compounds, particularly aluminides, are emerging as materials for high temperature structural applications. They promise to bridge the gap between the operating temperature range of structural ceramics and nickel-based superalloys. Recent investigations [1,2] have shown that iron aluminide alloys based on FeAl exhibit excellent resistance to oxidation, sulfidation and carburization. In comparison with nickel aluminides, iron aluminides are not high temperature materials. Nevertheless, they are candidate materials for use at moderate to high temperatures. However, they have generally low strength and poor creep resistance at these temperatures. Fortunately, mainly due to the efforts at the Oak Ridge National Laboratory, alloying with elements such as Mo, Zr, Nb, B, C etc., combined with appropriate processing procedures, has been shown [1–5] to lead to significant improvements in these properties. It is necessary to understand the influence of alloying additions and processing on the high temperature strength. The temperature dependence of the yield strength of FeAl is known [6,7] to be anomalous in the approximate temperature range 600–850 K. The high vacancy concentration that could result during cooling from high temperatures [8–11] or the increased difficulty of climb of ⟨111⟩ dislocations with temperature as proposed by Morris [12] may be responsible for this anomaly. However, it is at temperatures higher than the peak flow stress temperature that these alloys are expected to be processed and used in many applications. Investigations on the temperature and strain rate dependence of the flow stress in FeAl beyond the peak flow stress temperature have been very limited. Baker et al. [13] reported the yield stress variation with temperature up to 900 K in an off-stoichiometric FeAl strained at 10^{-4} s^{-1}. Maziasz et al. [1] presented yield strength data on cast FeAl from room

* Corresponding author. Tel.: +1-804-2749468; fax: +1-804-2744778.
E-mail address: dsastry@metalrg.iisc.ernet.in (D.H. Sastry).

0921-5093/01/$ - see front matter © 2001 Elsevier Science B.V. All rights reserved.
PII: S0921-5093(00)01380-0

temperature to 800°C and on hot extruded FeAl up to 1000°C. The effect of Y_2O_3 dispersion on the strength of Fe–40Al has been the subject of investigation [14] at temperatures up to 1000°C at a strain rate of 3×10^{-4} s^{-1} but the focus has been on the mechanism of particle strengthening. A higher temperature range (1100–1400 K) was investigated by Whittenberger [15,16] with particular reference to the effect of aluminum content in the range 41.7–48.7%, by employing constant rate compression testing. He identified two deformation regimes with an '*n*' (inverse of the strain rate sensitivity factor '*m*') value of 6 in the high stress regime and with a value of 3 at low stresses. The strain rates were however in the creep regime. Kumar and Pang [17] examined the dependency of strength and ductility at elevated temperatures on a Fe–40Al–0.6C alloy but the investigation was limited to 750°C. Furthermore, the strength could also be a strong function of strain rate, which has important consequences in processing the material at high temperatures and practically no data exist in the literature on this important deformation aspect of FeAl.

The present investigation is therefore directed towards assessing the temperature and strain rate dependence of flow stress of an FeAl alloy. The focus has been on the flow stress (stress corresponding to different strains) rather than the yield stress since such data are extremely useful in the processing of the material by different forming techniques but are lacking in the literature on most of the intermetallics under development. Attention has been paid to the deformation behavior in the temperature range 1073–1423 K, and, at each temperature, a wide strain rate range 10^{-3}–100 s^{-1}, has been covered. The temperature range selected and the higher end of the strain rate range chosen are of special interest to deformation processing from an engineering point of view. Compression testing has been employed and the flow stress data derived as a function of temperature, strain rate and strain have been analyzed to gain an insight into the rate controlling mechanism operating during hot deformation.

2. Experimental

The material tested in this work was of the following composition, Fe–24Al–0.42Mo–0.1Zr–0.005B–0.11C–0.31O (all in wt.%). Bars were obtained by the extrusion of water atomized powder contained in a steel can at 1373 K. The can was evacuated to remove any trapped air and sealed. The powder can was heated to the extrusion temperature and extruded through a 18-mm-diameter die. The hot extrusion process consolidated the powder into fully dense material and caused recrystallization. The extruded product was also homogeneous and free from porosity and other defects. The microstructure of the hot extruded alloy in the transverse direction is shown in Fig. 1. The structure shows fairly equiaxed grains with an average diameter of 22 μm. The microstructure further reveals uniformly dispersed alumina particles. These oxide particles are a result of the water atomization that introduces a high level of oxygen into the powder [18].

Compression tests were carried out in a 100-kN servo-hydraulic DARTEC testing machine. Cylindrical samples of a height to diameter ratio of 1.5 were machined from the powder-extruded rods. Most of the samples tested had a diameter of 10 mm. Concentric grooves of 0.5-mm depth were engraved on the sample faces to facilitate retention of the lubricant during testing. A three-zone furnace with proportional temperature controller for each zone was used to maintain a large uniform temperature zone. The temperatures employed for testing were in the range 1073–1423 K at intervals of 50 K. During testing, the actual temperature of the specimen as well as the adiabatic temperature rise were measured using a thermocouple inserted in a 0.8-mm-diameter hole drilled at half its height to reach the center of the specimen. The actuator speeds were so varied through a computer software program as to achieve any desired constant true strain rate in the range 0.001–100 s^{-1}. All the samples were compressed to an engineering strain of 0.5. Microstructural observations were made on deformed samples on sections parallel to the compression axis, etching the samples with Keller's reagent. Grain size measurements were carried out by the linear intercept method.

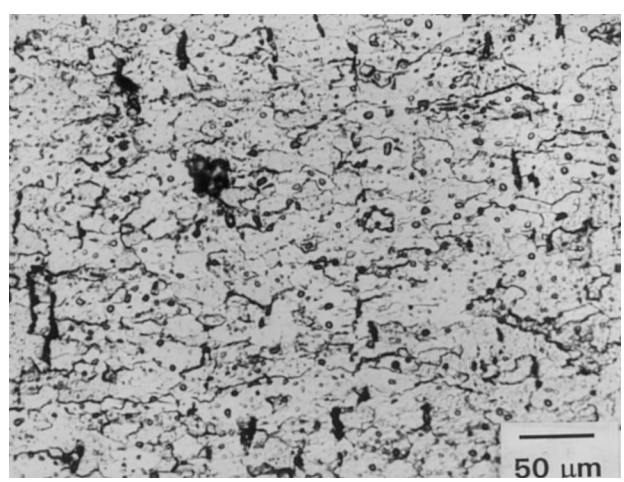

Fig. 1. Initial microstructure of the hot extruded water atomized P/M FeAl alloy.

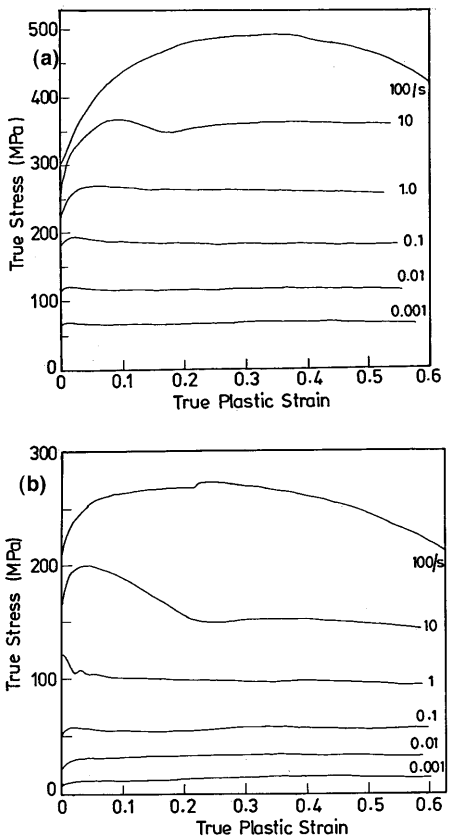

Fig. 2. True stress–true plastic strain curves for FeAl alloy deformed at (a) 1173 K and (b) 1373 K.

3. Results and discussion

3.1. Stress–strain behavior

The load-stroke data obtained in compression were processed to obtain true stress–true plastic strain curves using standard procedure. The flow stress data obtained at different temperatures, strain rates and strains were corrected for adiabatic temperature rise, if any, by linear interpolation of log σ versus $1/T$ data at constant rate, where σ is the flow stress and T the absolute temperature. This correction was found to be significant at lower temperatures and higher strain rates. Typical true stress–true plastic strain curves recorded at two selected temperatures, viz. 1173 and 1373 K are shown in Fig. 2. In general the curves at different temperatures may be broadly classified into two types depending on the strain rate. At strain rates lower than 1 s^{-1}, the curves are essentially of steady state type although an initial drop in the flow stress has occurred at temperatures higher than about 1223 K. At higher strain rates, however, the curves exhibit a peak in the yield stress at a strain which increases with strain rate. For a strain rate of 10 s^{-1}, the flow reaches a steady state only at large strains while at 100 s^{-1}, steady state is never reached in the strain range employed. Occasionally, oscillations in the stress–strain curves have been observed over a certain small range of strain at higher strain rates, for example at 1423 K and 1 s^{-1} over the approximate strain range 0.02–0.06.

3.2. Effect of temperature and strain rate

Fig. 3a and b describe the effect of temperature on the flow stress of the FeAl alloy at different strain levels. It can be seen that the flow stress at a given imposed strain rate depends on the temperature in a normal manner, decreasing with increase in temperature. The effect of strain rate is brought out more clearly in Fig. 4 where it is noticed that at a given temperature the flow stress increases with strain rate. Similar behavior is observed at other strains. Thus, the plastic flow behavior is seen to be thermally activated, the flow stress being a strong function of temperature and strain rate. However, the variation is less at low strain rates and at high temperatures. This means that, as is expected, it is beneficial in general to process the material under these conditions. The data are replotted in Fig. 5 in a more conventional way to bring out the effect of strain rate on the flow stress of the alloy as is normally done in creep studies. These log–log plots are linear (except at the lowest strain rate end) and are indicative of a power law relation between the stress

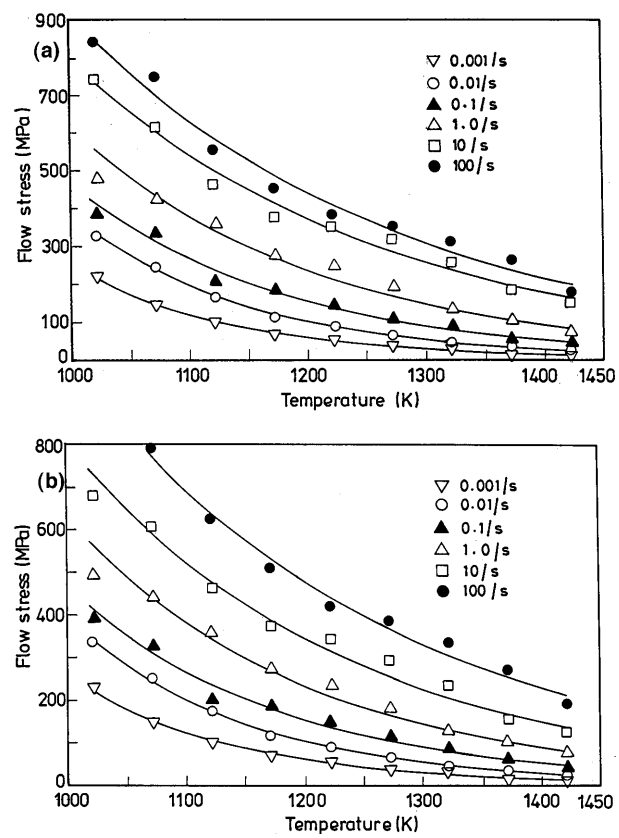

Fig. 3. Temperature and strain rate dependence of flow stress of FeAl alloy at (a) 0.1 strain and (b) 0.3 strain.

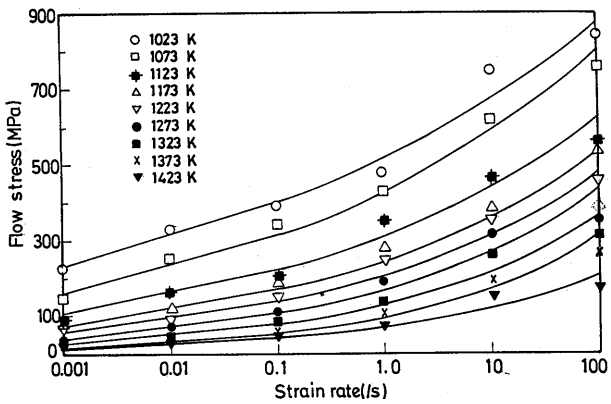

Fig. 4. Variation of flow stress of FeAl alloy with strain rate, typically shown at a strain of 0.1.

and strain rate which is a general observation in high temperature creep of materials. The stress exponent, n, for the strain rate can be estimated from the slopes of these plots:

$$n = \frac{\delta(\ln \dot{\varepsilon})}{\delta(\ln \sigma)} = \frac{1}{m} \tag{1}$$

where σ is the flow stress, $\dot{\varepsilon}$ the strain rate and m is known as the strain rate sensitivity. The values of n are included in Table 1. In the temperature range 1073–1373 K, n lies in the range 7.0–4.0 decreasing with temperature. At 1423 K, however, the magnitude of n is dependent of the strain rate; the lower strain rate range results in a value of n about 3.3. These values are fairly independent of the strain level in the range 0.1–0.5.

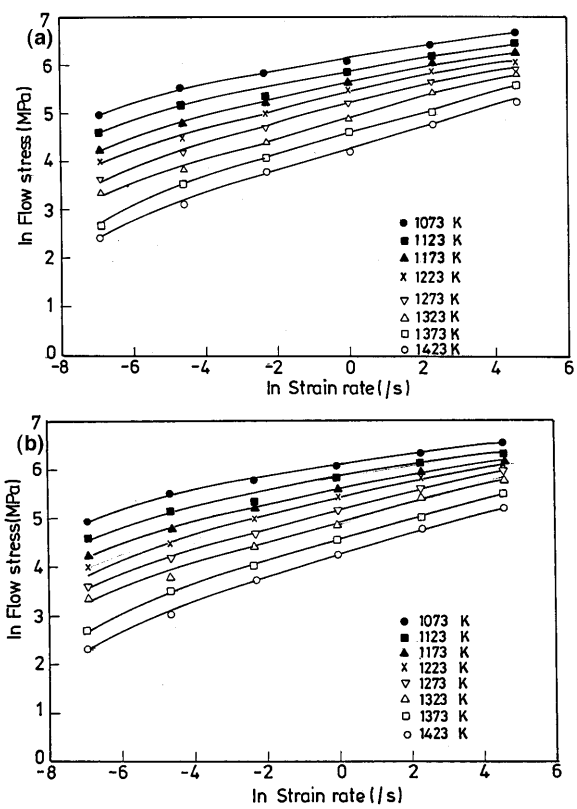

Fig. 5. Plots describing the strain rate sensitivity of flow stress in FeAl alloy at two strain levels: (a) 0.3 and (b) 0.5.

3.3. Thermal activation parameters

As stated earlier, the experimental data contained in Figs. 3 and 4 indicate that the plastic flow of FeAl alloy is thermally activated in the temperature and strain rate ranges employed in this investigation. Furthermore, since a power law behavior is noticed as seen from Fig. 5, it is appropriate to represent the experimental data by the classical Dorn type Arrhenius equation:

$$\dot{\varepsilon} = A\sigma^n \exp\left(\frac{-Q}{kT}\right) \tag{2}$$

where A is a constant, Q an apparent activation energy for deformation and k the Boltzmann constant. The activation energy is an important parameter on which an identification of the rate determining deformation mechanism is usually based. It has been evaluated in two ways. Firstly, in view of Eq. (2) and with a knowledge of the stress exponent, n, a plot of $\ln \sigma$ vs. $1/T$ at a constant strain rate yields a straight line with a slope of (Q/nk) from which Q can be computed. In the second method, the data of Fig. 5 are used. At a constant stress, the variation of $\ln \dot{\varepsilon}$ at a constant stress with $1/T$ is plotted, as in Fig. 6, to yield a slope of $-Q/k$ from which Q is calculated. Both methods of estimation yielded the same activation energy data. It is found that Q varies from about 430 kJ mol^{-1} in the stress range 44.7–148.4 MPa to 340 kJ mol^{-1} at high stresses, 99.5–270.4 MPa. Although some stress/temperature dependence of the activation energy is observed, it must be stated that the activation energy is fairly independent of strain rate and strain. If we focus our attention to the data only at 1373–1423 K, and at low strain rates (0.001–0.1 s^{-1}), a stress exponent n of about 3.3 is obtained with an associated activation

Table 1
Stress exponent in the Dorn equation for plastic flow of FeAl alloy as a function of temperature and strain

T, K	'n' at a true plastic strain of		
	0.1	0.3	0.5
1073	7.0	7.0	7.1
1123	6.6	6.6	6.6
1173	6.0	6.0	6.0
1223	5.5	5.4	5.5
1273	5.0	5.0	5.0
1323	4.5	4.6	4.7
1373	4.0	4.0	4.5
1423 ($\dot{\varepsilon} \geq 1$ s^{-1})	4.5	4.1	4.0
($\dot{\varepsilon} \leq 0.1$ s^{-1})	3.5	3.3	3.2

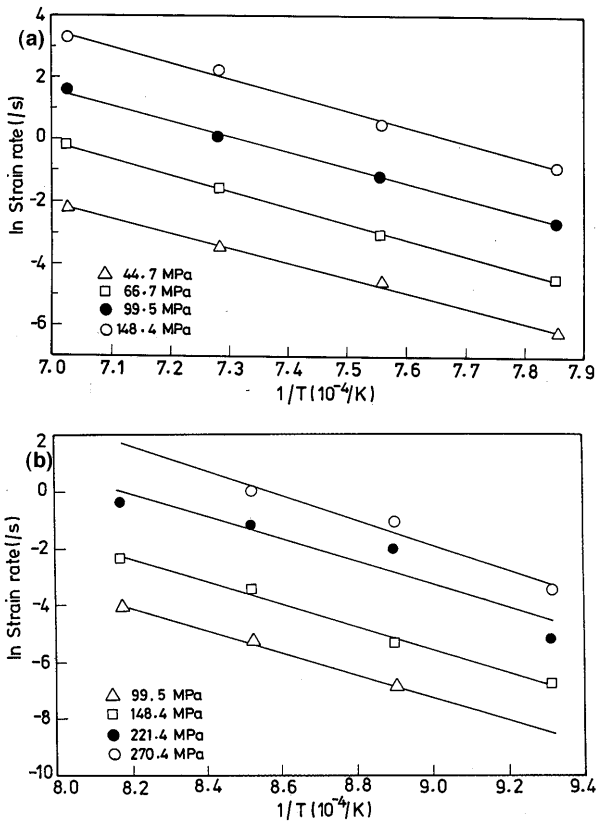

Fig. 6. Arrhenius plots to determine the activation energy for plastic flow, (a) at high temperatures/low stresses and (b) low temperatures/high stresses.

energy of 365 kJ mol^{-1} which falls in the range of Q expressed earlier.

It is of interest to compare the above activation energy values with those of other workers. The present high temperature/low stress Q value of 430 kJ mol^{-1} is in fair agreement with that (450 kJ mol^{-1}) obtained by Whittenberger [15,16] in a similar temperature range. The other data available in the literature mostly pertain to creep studies, i.e. low strain rate data. Tassa et al. [19] measured the steady state creep activation energy from tensile tests in the temperature range 1223–1373 K in two FeAl alloys. The resultant 'n' was 4.6 at 1223 K and 3.9 at 1373 K. The value of Q was about 452 kJ mol^{-1}, which was the same as that measured by Whittenberger. Sauthoff and coworkers [20–23] investigated the creep characteristics of (Fe,Ni)Al alloys with varying Fe/Ni ratio. They obtained a value of 3.5 for n and Q was found to lie between 270 and 350 kJ mol^{-1} for different alloys. However, the strain rate investigated by them was two to six orders of magnitude lower than the lowest value (0.001 s^{-1}) employed here and a direct comparison of the two sets of data may not be appropriate. Recently, Reimann and Sauthoff [24] examined the deformation behavior of FeAl as a function of aluminum content in the temperature range 873–1273 K by employing compression testing. They have measured a value of n for steady state creep in the range 4–5 and an apparent creep activation energy in the range 350–420 kJ mol^{-1} for most cases (different Al contents and different temperatures). It is clear that the present data are in good agreement with the results of Reimann and Sauthoff [24].

Another useful activation parameter which aids the determination of the operating deformation mechanism is an apparent activation area, A^*, for dislocation motion which is defined as:

$$A^* = \left(\frac{1}{b}\right) kT \left(\frac{\delta \ln \dot{\varepsilon}}{\delta \sigma}\right) \tag{3}$$

where b is the Burgers vector of the gliding dislocations. Here the flow shear stress must be substituted for σ and is taken as half the normal stress. Taking a value of 0.291 nm for b for $\langle 100 \rangle$ slip, the activation area for the high temperature deformation (1073–1373 K) of the present alloy is estimated from Eq. (3) to be about $160b^2$ at low stresses and $45b^2$ at high stresses. While the apparent activation area is seen to be a function of stress — it decreases with stress — it is found to be almost independent of temperature and strain. Stress change or strain rate change experiments yield more precise values of activation area than calculations based on data from plain stress–strain curves. However, Reimann and Sauthoff [24] also made measurements of activation area in FeAl as a function of aluminum content and temperature employing strain rate change and stress relaxation tests. Although their data show a lot of scatter, it is of interest to note that at the highest test temperature (1173 K) employed by them which falls in the temperature range investigated here, A^* is in the range $125–65b^2$ which again agrees well with the present data. Their data show a clear dependence of A^* on temperature, it increases with increasing temperature. However, this may only be a reflection of the dependence of A^* on stress since higher the temperature, lower is the stress to maintain the same steady state creep rate.

3.4. Deformation mechanism

As stated earlier, the material contained a dispersion of oxide particles. The particle size range was 50–500 nm and the approximate volume fraction was 10%. This dispersion was inherent in the method of preparation. The exact role of the dispersed particles on the mechanical behavior and processing is under investigation. However, the alloy seems to exhibit a moderately high strength at these temperatures. We now turn our attention to the possible rate-controlling mechanism operative during high temperature deformation of this FeAl alloy, excluding the temperature region near 1423 K and the strain rate range 0.001–0.1 s^{-1} which will be considered separately. The range of values of Q ob-

tained (430–340 kJ mol^{-1}) below 1373 K will first be considered. Since the change in the stress exponent, n, with temperature is gradual over the temperature range (Table 1), the experimental range of Q may not suggest the operation of different mechanisms in different temperature/stress regimes. It is likely that the change in Q (and also possible in n) is a manifestation of the variation of the material constant A in Eq. (2) with temperature and/or stress. The gradual variation of the flow stress with temperature in the entire temperature range (Fig. 3), the smooth variation of flow stress with the strain rate in the entire strain rate range (Fig. 4), the similar appearance of the stress–strain curves at all test temperatures and a gradual variation of 'n' with temperature lead us to postulate that only a single mechanism is strain rate controlling in the overall temperature range. For the purpose of this discussion, a middle value of 375 kJ mol^{-1} may be assumed for Q. It is evident that this is much higher than the activation energy of 265 kJ mol^{-1} for the diffusion of iron in FeAl [25]. However, this 'average' Q is closer to the activation energy for diffusion of Al in the B2 Fe–Al alloys [26]. It is of interest to note that an activation energy value of 375 kJ mol^{-1} was obtained for creep of Fe_3Al in the B2 phase field — the present alloy too has B2 structure — and was interpreted in terms of a diffusion mechanism [27]. Based on similar activation energy data, Reimann and Sauthoff [24] and Lin [28] have concluded that a diffusion mechanism involving climb of dislocations and formation of subgrains controls the creep/superplastic deformation behavior at high temperatures. It must be noted that dynamic recrystallization was observed [29] at high stain rates (≥ 1.0 s^{-1}) in the temperature range 1273–1423 K. Furthermore, flow softening is noticed in the stress–strain curves at high strain rates (Fig. 2). This characteristic is a pointer to infer that the alloy has a somewhat low stacking fault energy. In low stacking fault energy materials, the dynamic recrystallization process is nucleation-controlled [30,31] which means that dislocations are generated and simultaneously recovered by dislocation climb process. This process is clearly diffusion-controlled. It thus appears that the plastic flow of FeAl alloy in the temperature and strain rate range under discussion is diffusion-controlled, probably by the climb of dislocations.

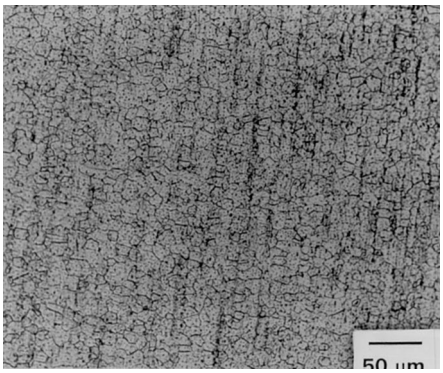

Fig. 7. Microstructure of FeAl alloy sample deformed in the superplastic domain of temperature and strain rate, 1373 K/0.1 s^{-1}.

Finally, the lower strain rate region (≤ 0.1 s^{-1}) around 1423 K will be considered. It may be recalled that a value of 3.3 was obtained for 'n'. This yields a strain rate sensitivity, m, value of 0.3 which is indicative of superplastic behavior. In fact the experimental results have indicated that at the lowest strain rate of 0.001 s^{-1}, m is 0.37. Values of m in the range 0.30–0.45 were reported by Lin [28] for the superplastic deformation of FeAl and its alloys at 1173 and 1273 K. The activation energy measured was 370 kJ mol^{-1} which is the same (365 kJ mol^{-1}) as that obtained in the present work. Superplasticity process requires diffusion-accommodated flow for which again the activation energy should be the activation energy for diffusion. The measured value of Q under superplastic conditions agrees well with the activation energy for diffusion of Al in FeAl. Fig. 7 shows a typical microstructure of the specimens deformed under superplastic conditions. It shows fine recrystallized grains and the grain size is almost independent of deformation temperature and strain rate. This fine grain size formed early in the deformation is stable over large deformations and is responsible for superplastic behavior in the range 1373–1423 K and in the strain rate range 0.001–0.1 s^{-1}. These temperature and strain rate regimes are ideal for manufacturing FeAl alloy components by superplastic forming with the most favorable parameters being 1423 K and 0.001 s^{-1} [29].

4. Summary and conclusions

The plastic flow behavior of a P/M FeAl alloy has been studied in the temperature range 1073–1423 K and in the strain rate range 0.001–100 s^{-1} by employing compression testing. At all temperatures, the stress–strain curves exhibit a steady state at strain rates lower than 1 s^{-1} and at higher strain rates a peak in the flow stress at a strain which increases with strain rate. The flow stress has been found to be strongly dependent upon the temperature and strain rate. The stress exponent n for the strain rate is in the range 7.0–4.0, decreasing with temperature. An apparent activation energy for deformation is estimated to be in the range 340–430 kJ mol^{-1}. The activation area is seen to be a function of stress and is in the range $160–45b^2$. At 1423 K however at strain rates lower than 0.1 s^{-1}, the value of n is 3.3 which is indicative of superplastic deformation behavior and the activation energy here is measured to be 365 kJ mol^{-1}. These activation

parameters are fairly independent of strain up to the true plastic strain of 0.5. The experimental data taken together suggest that a diffusion mechanism controls the rate of high temperature plastic flow in this FeAl alloy. The material can be processed by superplastic forming in the range 1373–1423 K at strain rates lower than 0.1 s^{-1}.

Acknowledgements

The authors are grateful to S. Sashidhara, R. Ravi and D. Mollaiah for their willing assistance in the experimental work. Thanks are due to Amy Solana for her generous help in the preparation of the figures and in the calculations. One of the authors (DHS) is grateful to Philip Morris, USA and Chrysalis Technologies Inc. for providing financial support for carrying out this work.

References

[1] P.J. Maziasz, G.M. Goodwin, D.J. Alexander, S. Viswanathan, in: S.C. Deevi, V.K. Sikka, P.J. Massiasz, R.W. Cahn (Eds.), Proceedings of International Symposium on Nickel and Iron Aluminides — Processing, Properties and Applications, ASM International, 1997, p. 157, 283.
[2] S.C. Deevi, V.K. Sikka, Intermetallics 4 (1996) 357.
[3] P.J. Masiasz, C.T. Liu, G.M. Goodwin, in: K. Natesan, P. Ganesan, G. Lai (Eds.), Heat Resistant Materials II, ASM International, 1995, p. 555.
[4] P.J. Masiasz, D.J. Alexander, J.L. Wright, Intermetallics 5 (1997) 547.
[5] C.T. Liu, E.P. George, P.J. Masiasz, J.H. Schneibel, Mater. Sci. Eng. A258 (1998) 84.
[6] K. Yoshimi, S. Hanada, M.H. Yoo, Acta Metall. 43 (1995) 4141.
[7] H.E. Schafer, B. Damson, M. Weller, E. Arzt, E.P. George, Phys. Stat. Sol. a160 (1997) 531.
[8] M.A. Morris, O. George, D.G. Morris, Mater. Sci. Eng. A258 (1998) 99.
[9] I. Baker, P. Nagpal, in: R. Darolia, et al. (Eds.), Structural Intermetallics, TMS, 1993, p. 463.
[10] R. Carlton, E.P. George, R.H. Zee, Intermetallics 3 (1995) 433.
[11] E.P. George, I. Baker, Phil. Mag. A77 (1998) 737.
[12] D.G. Morris, Phil. Mag. 71 (1995) 1281.
[13] I. Baker, H. Xiao, O. Klein, C. Nelson, J.D. Whittenberger, Acta Metall. Mater. 43 (1995) 1723.
[14] D.G. Morris, in: S.C. Deevi, V.K. Sikka, P.J. Massiasz, R.W. Cahn (Eds.), Proceedings of International Symposium on Nickel and Iron Aluminides — Processing, Properties and Applications, ASM International, 1997, p. 73.
[15] J.D. Whittenberger, Mater. Sci. Eng. 57 (1983) 77.
[16] J.D. Whittenberger, Mater. Sci. Eng. 77 (1986) 103.
[17] K.S. Kumar, L. Pang, Mater. Sci. Eng. A258 (1998) 153.
[18] M.R. Hajaligol, S.C. Deevi, V.K. Sikka, C.R. Scorey, Mater. Sci. Eng. A258 (1998) 249.
[19] O. Tassa, C. Testani, B. Ricci Bitti, Scr. Met. Mater. 26 (1992) 1813.
[20] M. Rudy, G. Sauthoff, Mater. Sci. Eng. 81 (1986) 525.
[21] I. Jung, M. Rudy, G. Sauthoff, Mater. Res. Symp. Proc. 81 (1987) 263.
[22] I. Jung, G. Sauthoff, Z. Metallk. 80 (1989) 484.
[23] M. Rudy, G. Sauthoff, Mater. Res. Symp. Proc. 39 (1987) 27.
[24] U. Reimann, G. Sauthoff, Intermetallics 7 (1999) 437.
[25] M. Eggersmann, B. Sepiol, G. Vogl, H. Mehrer, Defect Diffusion Forum 339 (1997) 143.
[26] E. Kentzinger, M.C. Cadeville, V. Pierron-Bohnes, W. Petry, B. Hennion, J. Phys. Condens. Matter 8 (1996) 5535.
[27] R.S. Sundar, Ph.D. Thesis, Indian Institute of Science, Bangalore, 1998.
[28] D. Lin, in: S.C. Deevi, V.K. Sikka, P.J. Massiasz, R.W. Cahn (Eds.), Proceedings of International Symposium on Nickel and Iron Aluminides — Processing, Properties and Applications, ASM International, 1997, p. 187.
[29] Y.V.R.K. Prasad, D.H. Sastry, S.C. Deevi, Paper presented at the Symposium on Intermetallics for the Third Millennium, November 1–4, ASM, Cincinnati, 1999.
[30] B. Derby, M.F. Ashby, Scr. Metall. 21 (1987) 879.
[31] Y.V.R.K. Prasad, N. Ravichandran, Bull. Mater. Sci. 14 (1991) 1241.